AIDA-2020-PUB-2016-013

AIDA-2020

Advanced European Infrastructures for Detectors at Accelerators

Journal Publication

Free carrier absorption in self-activated PbWO_4 and Ce-doped Y_3(Al_0.25Ga_0.75)_3O_12 and Gd_3Al_2Ga_3O_12 garnet scintillators

E. Auffray (CERN) *et al*

14 August 2016

The AIDA-2020 Advanced European Infrastructures for Detectors at Accelerators project has received funding from the European Union's Horizon 2020 Research and Innovation programme under Grant Agreement no. 654168.

This work is part of AIDA-2020 Work Package **14: Infrastructure for advanced calorimeters**.

The electronic version of this AIDA-2020 Publication is available via the AIDA-2020 web site <http://aida2020.web.cern.ch> or on the CERN Document Server at the following URL: <http://cds.cern.ch/search?p=AIDA-2020-PUB-2016-013>

Free Carrier Absorption in Self-Activated $PbWO_4$ and Ce-doped $Y_3(Al_{0.25}Ga_{0.75})_3O_{12}$ and $Gd_3Al_2Ga_3O_{12}$ garnet scintillators

E. Auffray[a], M. Korjik[b], M.T. Lucchini[a], S. Nargelas[c], O. Sidletskiy[d], G. Tamulaitis[c], Y. Tratsiak[e*], A. Vaitkevičius[c]

[a] CERN, Geneva, Switzerland

[b] Research Institute for Nuclear Problems, Belarusian State University, Bobruiskaya str. 11, Minsk, Belarus

[c] Semiconductor Physics Department and Institute of Applied Research, Vilnius University, Universiteto str. 3, Vilnius, Lithuania

[d] Institute for Scintillation Materials, Lenin av. 60, Kharkov, Ukraine

[e] Research Institute for Chemical Problems, Belarusian State University, Leningradskaya str. 14, Minsk, Belarus

[*] Corresponding author: E-mail: slon.zhenya@gmail.com

Highlights:

- Free electrons are generated by short pulse in subpicoseconds in PWO and YAGG:Ce
- The relaxation of holes from Gd to valence band in GAGG:Ce takes 5-10 ps
- Hole trapping at Gd deteriorates response speed in mixed garnet scintillators

Keywords: Scintillators, free carrier absorption, lead tungstate, cerium-doped garnets.

Abstract

Nonequilibrium carrier dynamics in the scintillators prospective for fast timing in high energy physics and medical imaging applications was studied. The time-resolved free carrier absorption investigation was carried out to study the dynamics of nonequilibrium carriers in wide-band-gap scintillation materials: self-activated led

tungstate ($PbWO_4$, PWO) ant two garnet crystals, GAGG:Ce and YAGG:Ce. It was shown that free electrons appear in the conduction band of PWO and YAGG:Ce crystals within a sub-picosecond time scale, while the free holes in GAGG:Ce appear due to delocalization from Gd^{3+} ground states to the valence band within a few picoseconds after short-pulse excitation. The influence of Gd ions on the nonequilibrium carrier dynamics is discussed on the base of comparison the results of the free carrier absorption in GAGG:Ce containing gadolinium and in YAGG without Gd in the host lattice.

1. Introduction

The high-energy physics experiments in sight and advanced medical imaging devices based on positron emission tomography (PET), positron annihilation lifetime spectroscopy (PALS) and other techniques require fast scintillation detectors. Currently the best time resolution of scintillation detectors is at the limit of 100 ps: ~200 ps is reported for detectors based on LYSO:Ce [1] and PWO [2], a sub-100-ps coincidence time resolution is reported for PET with LSO:Ce,Ca scintillation detectors, while a sub-100-ps time resolution was measured with PWO-based detectors in the CMS ECAL experiments [3]. A 10-ps-resolution is the next target in development of scintillation detectors [4,5]. The current demand for faster timing of scintillation detectors used both in high luminosity high energy physics experiments and in medical applications inspire deeper studies of the dynamics of nonequilibrium carriers generated in scintillator material.

Recently, we investigated the carrier dynamics in $PbWO_4$ (PWO) and $Gd_3Al_2Ga_3O_{12}$:Ce (GAGG:Ce) using time-resolved photoluminescence technique [6]. In the current paper, a time-resolved free carrier absorption technique was exploited. Three scintillation materials have been under study: self-activated led tungstate ($PbWO_4$, PWO) and two cerium-doped garnets, GAGG and $Y_3Al_2Ga_3O_{12}$ (YAGG).

PWO exhibits short emission decay time and has good radiation hardness to γ quanta. In spite of a comparatively low light yield, 200 ph/MeV, PWO-based scintillators are used in the radiation detectors, which are currently being exploited in several high-energy physics experiments, including such large experiments as CMS and ALICE at LHC(CERN) [7] and future PANDA detector at FAIR (GSI, Germany) [8]. The predominant luminescence mechanism in PWO is emission via quenched

polaronic states, due to recombination of excitations on the host oxy-anionic complexes WO_4^{2-} [9,10].

Ce-doped yttrium and gadolinium aluminum gallium garnets, YAGG and GAGG, respectively, are an excellent example for engineering of the material luminescent properties [11].

The rise time of the luminescence response to short pulse excitation in GAGG:Ce was found to be in the range of several nanoseconds even at the direct resonant excitation of Ce^{3+} ions [6]. This feature was explained by taking into account possible carrier trapping at the sublattice of the host-building Gd^{3+} ions, which is in line with the excitation transfer from Gd^{3+} to Ce^{3+} studied in Gd_2SiO_5:Ce crystal [12]. A more detailed study of the role of Gd^{3+} subsystem in the energy transfer processes in garnet crystals plays important role in future optimization of these crystals for exploiting as scintillation material. In particular, scintillation crystals and phosphors based on mixed garnets doped with cerium attract considerable interest due to ability of manipulation with their luminescent and scintillation properties by changing the Al/Ga ratio in the compound [13]. This ability is enabled by the change in the strength of the crystal field acting on the activator ions and, consequently, by shifting the energy levels of Ce^{3+} relative to the bottom of the conduction band. Moreover, optimization of garnet composition serves also for the enhancement of the light yield of these scintillators [14]. The most impressive results have recently been achieved in GAGG:Ce, where the scintillation yield of up to 58000 ph/MeV was demonstrated both in single crystals and transparent ceramics [13,15].

After demonstration of the formation $Y_3Al_2Ga_3O_{12}$ (YAGG) via sol-gel synthesis [16] and the micro-pulling down method [17], this mixed garnet attracts considerable interest as host material for Ce-based phosphors and scintillators. YAGG:Ce might be used as green phosphor in light-emitting diodes with high color rendering [18]. Strong persistent green [19] and yellow [20] luminescence was also observed in $Y_3Al_2Ga_3O_{12}$:Ce ceramics co-activated with chromium ions [19,20]. In both garnets, GAGG and YAGG, the second and third Stark components of $4f^05d^1$ configuration of Ce^{3+} ion are located in the conduction band [20]. However, the host matrix of YAGG does not contain Gd^{3+} sublattice. Therefore, the comparison of Ce-doped GAGG and YAGG offers an informative insight into the influence of gadolinium on the dynamics of nonequilibrium carriers.

2. Samples

The PWO crystal under study was grown by Czochralski technique as described in more detail in [9]. The 2x2x0.1 cm^3 sample was prepared from the ingot of PWO-II quality [2].

$Y_3(Al_{0.25}Ga_{0.75})_3O_{12}$ and $Gd_3Al_2Ga_3O_{12}$ crystals doped with Ce were grown by Czochralski method from the melt containing 1 at.% of Ce in a slightly oxidized neutral atmosphere. The samples under study with dimensions 0.7x0.7x0.5 cm^3 were cut from the seed part of the ingots exhibiting higher optical quality. The light yield of YAGG:Ce was found to be by a factor of 7 smaller than that of GAGG:Ce.

3. Experimental

The measurements of free carrier absorption have been performed by using a femtosecond Yb:KGW laser PHAROS (Light Conversion Ltd.) emitting at 1030 nm. The laser produced 200 fs pulses at 30 kHz repetition rate. A part of the fundamental laser harmonic was frequency-quadrupled using β-barium borate crystals and the light at 254 nm (4.9 eV) was used as a pump beam for pulsed excitation of free carriers. The excitation beam was focused on the sample surface into a spot of ~350 μm in diameter. The remaining part of laser radiation at 1030 nm was delayed by an opto-mechanical delay line and used as a probe to follow the time evolution of the induced absorption, which is proportional to free carrier density. All measurements were performed at room temperature.

4. Results and discussion

4.1 Free carrier absorption in $PbWO_4$

The excitation at 254 nm corresponds to interband transitions in lead tungstate crystal. Figure 1 shows the decay of the excitation-induced free carrier absorption (FCA) in PWO crystal at different pulse energy densities of the excitation. The initial part of this decay is presented in Fig. 2. The increase in excitation intensity results in increased contribution of the fast decay component. The dependence of the peak induced absorption on excitation intensity is presented in Fig. 3 as the dependence of the induced absorption at the probe wavelength (1030 nm) on pump pulse energy

density. The optical density of the induced absorption in PWO and in other two samples under study (not shown) was found to be proportional to the energy density in a wide dynamic range, as expected for free carrier absorption. This evidence confirms the assumption that the probe absorption originates exclusively from the carriers created via pumping.

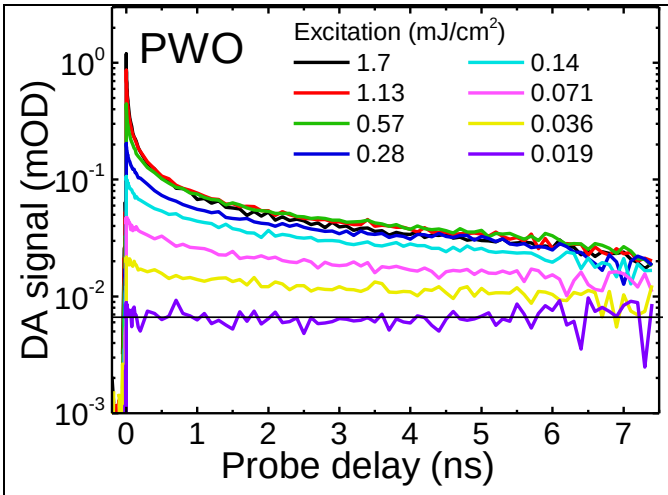

Fig. 1. Kinetics of optical density induced by short pulse excitation of PWO crystal at 254 nm, probed at 1030 nm, for different excitation pulse energy densities (indicated).

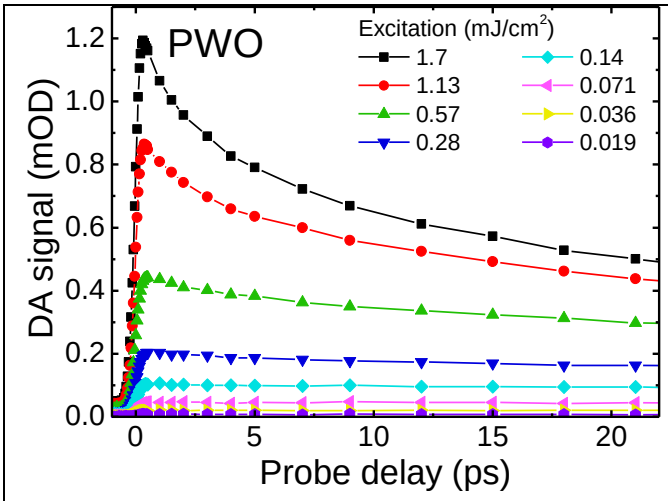

Fig. 2. Initial part of the kinetics presented in Fig. 1.

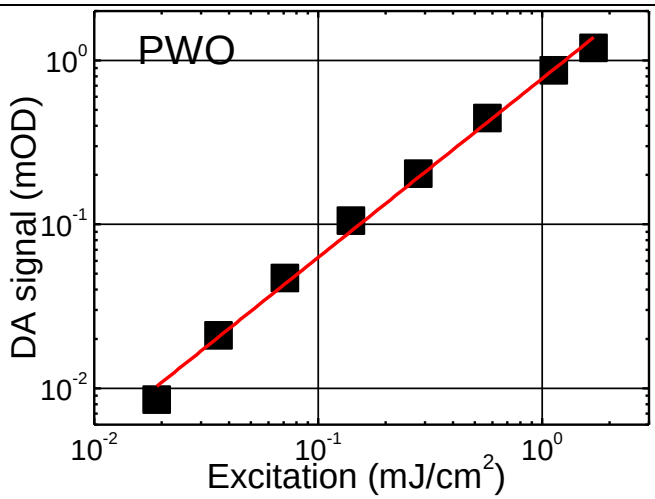

Fig. 3. Induced optical density at 1030 nm probe wavelength at 0.3 ps delay after short pump pulse at 254 nm versus pump pulse energy density.

The subpicosecond rise time of FCA at interband excitation in the self-activated luminescent lead tungstate is a clear indication that the nonequilibrium free electrons appear in the conduction band within subpicosecond time scale. This is in consistence with interpretation that the luminescent matrix-forming oxy-anionic complexes WO_4^{2-} provide conditions for formation of self-localized excitons. Furthermore, the FCA exhibits a respond kinetics, which correlates with the photoluminescence kinetics observed by us before [6].

The excitation at 254 nm generates free carriers in the PWO crystal in the subpicosecond domain. As the excitation density is increased, the probability of the non-germinal carrier recombination shows an increase resulting in acceleration of the initial part of the FCA decay. This effect was supported by our experimental results obtained with PWO sample.

4.2 Free carrier absorption in YAGG:Ce

The measured absorption spectrum of Ce^{3+} in YAGG:Ce crystal is similar to that reported before [21]: it contains three bands peaked at 448, 350, and 250 nm. Thus, pumping at 254 nm coincides pretty good with the upper, third, absorption band due to inerconfiguration electronic transition $4f^15d^0 \rightarrow 4f^05d^1$ of Ce^{3+} ions. Figure 4 shows FCA kinetics in YAGG:Ce crystal for different excitation energy densities at 254 nm. The initial part of the decay kinetics is depicted in Fig. 5. The kinetics consists of

three components. The fast and intermediate components have characteristic decay times of 2 ps and ~100 ps with no significant dependence on excitation intensity. The decay time of the slow decay component is in nanosecond domain and decreases down to a few nanoseconds as the excitation intensity increases.

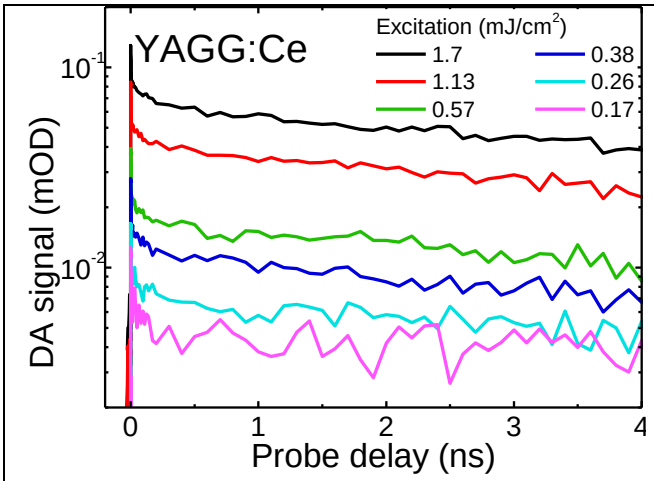

Fig. 4. Kinetics of optical density induced by short-pulse excitation of YAGG:Ce crystal at 254 nm for different excitation pulse energy densities (indicated).

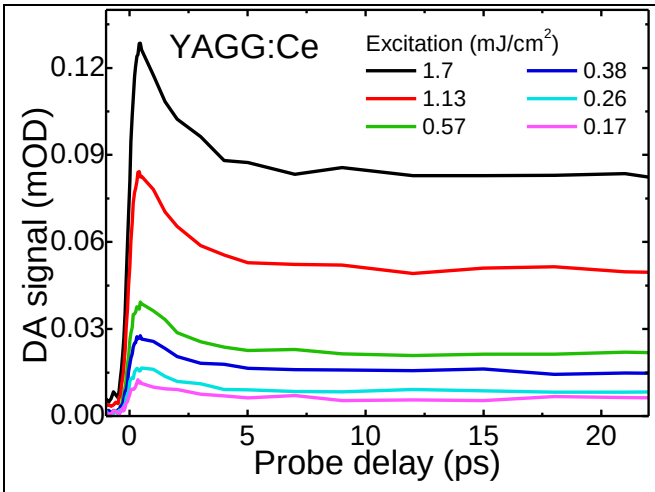

Fig. 5. Initial part of the kinetics presented in Fig. 4.

Since the excitation YAGG:Ce crystal with 4.9 eV (254 nm) photons corresponds to transition to the third Stark component of $4f^0 5d^1$ configuration in Ce^{3+} ions, and the edge of the conduction band in Al/Ga mixed garnets has energy near 6.2 eV (200 nm) [22], the wavelength of 254 nm corresponds to the predominant

excitation of Ce^{3+} ions. However, a fast delocalization of the electrons from Ce^{3+} is highly probable, since the excited state is within the conduction band. Thus, the initial FCA decay is, most probably, caused by fast delocalization within ~2 ps, the further kinetics of FCA with the decay time in the 100 ps range proceeds after the equilibrium among the processes of depopulation and repopulation of Ce^{3+} and recombination is established. The decay in the nanosecond time is influenced by capturing of electrons from the conduction band by traps due to shallow defect states, which are present in abundance in mixed garnets.

4.3 Influence of gadolinium on carrier dynamics in GAGG:Ce

Figure 6 shows the absorbance spectrum of GAGG:Ce crystal at room temperature. The spectrum consists of absorption bands due to $4f^15d^0 \rightarrow 4f^05d^1$ interconfiguration transitions of Ce^{3+} ions and $^8S \rightarrow {}^6P$, ^6I, ^6D intraconfiguration transitions of matrix-building gadolinium ions forming narrow subbands due to P, I, and D states. The absorption band corresponding to the transition to the third Stark component of $4f^05d^1$ configuration is shifted to short wavelength range in GAGG in comparison with that in YAGG. Therefore, the photons of 254 nm wavelength excite Ce^{3+} ion only into the long-wavelength shoulder of the absorption band due to the third inerconfiguration electronic transition $4f^15d^0 \rightarrow 4f^05d^1$ and Gd^{3+} subsystem directly via $^8S \rightarrow {}^6D$ transitions.

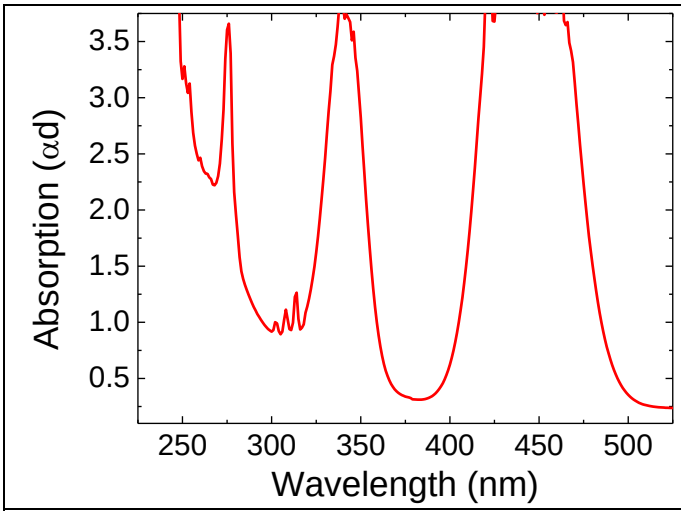

Fig. 6. Room temperature absorbance spectrum of GAGG:Ce.

Figures 7 and 8 show FCA kinetics in GAGG:Ce crystal at different excitation pulse energy densities at the wavelength of 254 nm in the range of nanoseconds and within the first 20 picoseconds after short-pulse excitation, respectively.

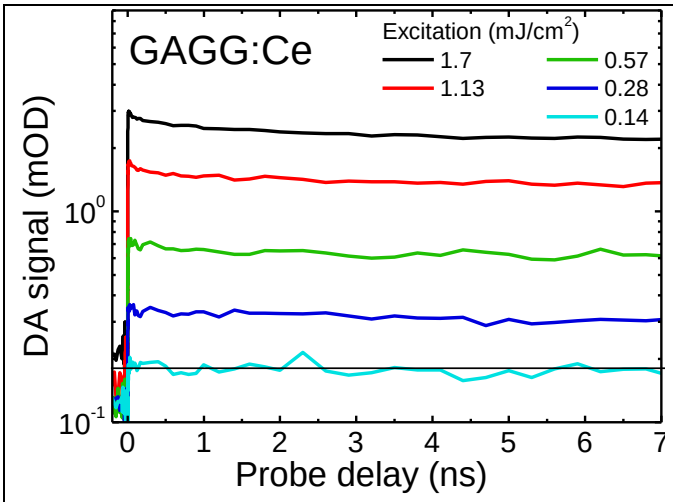

Fig. 7. Kinetics of optical density induced by short pulse excitation of GAGG:Ce crystal at 254 nm for different excitation pulse energy densities (indicated).

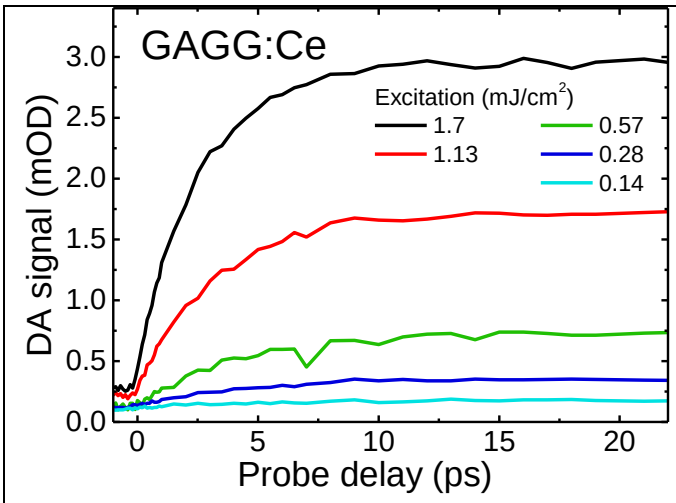

Fig. 8. Initial part of the kinetics presented in Fig. 7.

The FCA decay at low excitation intensities is monoexponential with the characteristic decay time substantially exceeding the time range under study (8 ns). The decay becomes increasingly nonexponential at elevated excitation intensities. The most interesting feature in the FCA response to a short pulse excitation is the rising part of the response. In contrast to PWO and YAGG:Ce, where the rise time is below the time resolution in our experiments (200 fs), the rise of the FCA response in GAGG:Ce is considerably slower. The rise time is approximately 10 ps at low

excitation of 0.14 mJ/cm^2 and decreases to 5 ps as the excitation is increased by an order of magnitude.

For GAGG:Ce scintillating crystals, the excitation with 4.9eV (254 nm) photons corresponds to $^8S \rightarrow {}^6D_{7/2,9/2}$ transition of Gd^{3+} ions and a weak excitation into the long wavelength wing of the band corresponding to transition to the third Stark component of $4f^05d^1$ Ce^{3+} electronic configuration. Similarly to YAGG crystal, the band gap due to p→d interband transitions has energy near 6.2 eV (200 nm) [22], thus, the wavelength of 254 nm corresponds to the predominant excitation of Gd^{3+} ions. Consequently, electrons do not appear in the conduction band due to this transition. Thus, the FCA signal we observed here is due to absorption by free holes, which are released from Gd^{3+} ^8S ground state into the valence band. This assumption is in good agreement with the analysis performed by P. Dorenbos [23], showing that the ground state of Gd^{3+} in $4f^7$ shell is localized in the valence band. The rise of FCA, which takes a few picoseconds, is caused by delocalization of holes from Gd^{3+} to valence band. When the hole is localized at the Gd^{3+} f-level, its direct transfer by absorption of photons to p orbitals, forming the top of valence band is forbidden. However, the transition might occur via mixed p-d orbitals in the valence band. This relaxation takes 5-10 ps, depending on the density of nonequilibrium holes, which is observed as the rise time in FCA experiments. The decay of FCA kinetics proceeds rather slow in comparison with that in PWO and YAGG:Ce, with the characteristic decay time of 1 ns even at the first decay stages and even more slowly afterwards. This time is required for the hole to be captured from the valence band by Ce^{3+} ion. This interpretation is consistent with the published observation that the luminescence rise time in GAGG:Ce equals several nanoseconds [6].

5. Conclusions

The time resolved study of free carrier absorption in three scintillation materials, self-activated PWO and cerium-doped GAGG and YAGG showed that the free electrons are instantaneously generated into the conduction band under band-to-band excitation of PWO and at the excitation to the third Stark component of $4f^05d^1$ Ce^{3+} configuration forming a state in the conduction band. Meanwhile in GAGG:Ce, a substantially slower relaxation of free carrier absorption was observed and attributed

to the absorption by free holes. Moreover, the rise of FCA in GAGG:Ce, takes a few picoseconds, what is caused by delocalization of holes from Gd^{3+} to valence band. This observation is consistent with the conclusion reported in [23] that the ground state of the $^{8}S \rightarrow {}^{6}D_{7/2,9/2}$ intracenter transition of Gd^{3+} ions is located within the valence band. The results show that the hole trapping at Gd sublattice is an important factor deteriorating response rise in scintillators based on mixed garnets containing gadolinium.

Acknowledgement

This work has been carried out in line with the targets of Crystal Clear Collaboration and supported by H2020-INFRAIA-2014-2015 project no. 654168 (AIDA-2020). Authors are grateful to COST Action TD1401 "Fast Advanced Scintillator Timing (FAST)" for support of collaboration.

References

[1] D.N. ter Weele, D.R. Schaart, P. Dorenbos, Intrinsic scintillation pulse shape measurements by means of picosecond x-ray excitation for fast timing applications, Nucl. Instruments Methods Phys. Res. Sect. A Accel. Spectrometers, Detect. Assoc. Equip. 767 (2014) 206–211. doi:10.1016/j.nima.2014.08.019.

[2] M. Kavatsyuk, D. Bremer, V. Dormenev, P. Drexler, T. Eissner, W. Erni, et al., Performance of the prototype of the Electromagnetic Calorimeter for PANDA, Nucl. Instruments Methods Phys. Res. Sect. A. 648 (2011) 77–91. doi:10.1016/j.nima.2011.06.044.

[3] CMS Collaboration, Time Reconstruction and Performance of the CMS Electromagnetic Calorimeter, J. Instrum. 5 (2010) T03011. doi:10.1088/1748-0221/5/03/T03011.

[4] P. Lecoq, M. Korzhik, A. Vasiliev, Can Transient Phenomena Help Improving Time Resolution in Scintillators, IEEE Trans. Nucl. Sci. 61 (2014) 229–234. doi:10.1109/TNS.2013.2282232.

[5] E. Auffray, O. Buganov, a Fedorov, M. Korjik, P. Lecoq, G. Tamulaitis, et al., New detecting techniques for a future calorimetry, J. Phys. Conf. Ser. 587 (2015) 012056. doi:10.1088/1742-6596/587/1/012056.

[6] E. Auffray, R. Augulis, A. Borisevich, V. Gulbinas, A. Fedorov, M. Korjik, et al., Luminescence rise time in self-activated PbWO4 and Ce-doped Gd3Al2Ga3O12 scintillation crystals, J. Lumin. in press (2016). doi:10.1016/j.jlumin.2016.05.015.

[7] A. Breskin, R. Voss, eds., The CERN large hadron collider: accelerator and experiments, CERN, Geneva, 2009.

[8] H.H. Gutbrod, I. Augustin, H. Eickhoff, K.-D. Groß, W.F. Henning, D. Krämer, et al., eds., FAIR - Baseline Technical Report, Vol.1, Gesellschaft für

Schwerionenforschung mbH, Darmstadt, 2006.

[9] A.A. Annenkov, M. V. Korzhik, P. Lecoq, Lead tungstate scintillation material, Nucl. Instruments Methods Phys. Res. Sect. A Accel. Spectrometers, Detect. Assoc. Equip. 490 (2002) 30–50. doi:10.1016/S0168-9002(02)00916-6.

[10] M. Nikl, P. Bohacek, E. Mihokova, M. Kobayashi, M. Ishii, Y. Usuki, et al., Excitonic emission of scheelite tungstates AWO4 (A = Pb, Ca, Ba, Sr), J. Lumin. 87 (2000) 1136–1139. doi:10.1016/S0022-2313(99)00569-4.

[11] K. Kamada, T. Endo, K. Tsutumi, T. Yanagida, Y. Fujimoto, A. Fukabori, et al., Composition Engineering in Cerium-Doped (Lu,Gd)3(Ga,Al)5O12 Single-Crystal Scintillators, Cryst. Growth Des. 3 (2011) 4484–4490. doi:10.1021/cg200694a.

[12] D.M. Kondratiev, M. V. Korzhik, A.A. Fyodorov, V.B. Pavlenko, Scintillation in cerium-activated gadolinium-based crystals, Phys. Status Solidi. 197 (1996) 251–258. doi:10.1002/pssb.2221970132.

[13] K. Kamada, S. Kurosawa, P. Prusa, M. Nikl, V. V. Kochurikhin, T. Endo, et al., Cz grown 2-in. size Ce:Gd3(Al,Ga)5O12 single crystal; relationship between Al, Ga site occupancy and scintillation properties, Opt. Mater. (Amst). 36 (2014) 1942–1945. doi:10.1016/j.optmat.2014.04.001.

[14] O. Sidletskiy, A. Gektin, A. Belsky, Light-yield improvement trends in mixed scintillation crystals, Phys. Status Solidi. 211 (2014) 2384–2387. doi:10.1002/pssa.201431137.

[15] N.J. Cherepy, Z.M. Seeley, S.A. Payne, P.R. Beck, O.B. Drury, S.P. O'Neal, et al., Development of transparent ceramic Ce-doped gadolinium garnet gamma spectrometers, IEEE Trans. Nucl. Sci. 60 (2012) 2330 – 2335. doi:10.1109/NSSMIC.2012.6551400.

[16] I. Muliuoliene, S. Mathur, D. Jasaitis, H. Shen, V. Sivakov, R. Rapalaviciute, et al., Evidence of the formation of mixed-metal garnets via sol-gel synthesis, Opt. Mater. (Amst). 22 (2003) 241–250. doi:10.1016/S0925-3467(02)00271-9.

[17] K. Kamada, T. Yanagida, J. Pejchal, M. Nikl, T. Endo, K. Tsutumi, et al., Scintillator-oriented combinatorial search in Ce-doped (Y,Gd)3(Ga,Al)5O12 multicomponent garnet compounds, J. Phys. D. Appl. Phys. 44 (2011) 505104. doi:10.1088/0022-3727/44/50/505104.

[18] Y. Qiang, Y. Yu, G. Chen, J. Fang, Synthesis and luminescence properties of Y2.94Al5−mGamO12:0.06Ce3+ (1≤m≤2.5) green phosphors for white LEDs, Ceram. Int. 42 (2016) 767–773. doi:10.1016/j.ceramint.2015.09.001.

[19] J. Xu, S. Tanabe, A.D. Sontakke, J. Ueda, Near-infrared multi-wavelengths long persistent luminescence of Nd3+ ion through persistent energy transfer in Ce3+, Cr3+ co-doped Y3Al2Ga3O12 for the first and second bio-imaging windows, Appl. Phys. Lett. 107 (2015) 081903. doi:10.1063/1.4929495.

[20] J. Ueda, K. Kuroishi, S. Tanabe, Yellow persistent luminescence in Ce3+-Cr3+-codoped gadolinium aluminum gallium garnet transparent ceramics after blue-light excitation, Appl. Phys. Express. 7 (2014) 062201. doi:10.7567/APEX.7.062201.

[21] J. Ueda, K. Kuroishi, S. Tanabe, Bright persistent ceramic phosphors of Ce3+-Cr 3+-codoped garnet able to store by blue light, Appl. Phys. Lett. 104 (2014) 101904. doi:10.1063/1.4868138.

[22] J.M. Ogieglo, Luminescence and Energy Transfer in Garnet Scintillators, Utrecht University, 2012. http://dspace.library.uu.nl/handle/1874/257552.

[23] P. Dorenbos, A Review on How Lanthanide Impurity Levels Change with Chemistry and Structure of Inorganic Compounds, ECS J. Solid State Sci. Technol. 2 (2013) R3001–R3011. doi:10.1149/2.001302jss.